

Application of graph theory and topological models for the determination of fundamentals of the aromatic character of pi-conjugated hydrocarbons*

Michał K. Cyrański^{1,‡}, Arkadiusz Ciesielski^{1,2},
Tadeusz M. Krygowski¹, and Dorota K. Stępień¹

¹*Department of Chemistry, University of Warsaw, Pasteura 1, 02-093 Warsaw, Poland;* ²*Institute of Biochemistry and Biophysics, Polish Academy of Science, Pawlowskiego 5a, 02-106 Warsaw, Poland and Department of Chemistry, University of Warsaw, Pasteura 1, 02-093 Warsaw, Poland*

Abstract: Application of topological analysis and graph theory to benzenoid hydrocarbons leads to the determination of fundamentals of aromaticity: the Hückel rule and the Clar rule. The approach, based on a treatment of the adjacency matrix, allows resonance energy (RE)-like characteristics to be estimated with quite good accuracy, and magnetic aromaticity indices to be derived for both the individual rings and the whole molecules. It also allows an effective approach for interpreting ring current formation in molecules when exposed to an external magnetic field. The transformation of the perturbation matrix into a form describing the canonical structures allows their gradation and determination of their stabilizing/destabilizing character.

Keywords: aromaticity; graph theory; topological models.

INTRODUCTION

Both the graph theory and topological models have long been used for modeling chemical and physico-chemical properties of chemical compounds [1–4]. The history of the graph theory began with the famous L. Euler problem of the seven bridges of Königsberg [5] but since then developed extensively and found applications in numerous fields of human activity [6–8]. In the simplest way, graph theory allows chemical species to be presented as a collection of edges and vertices, which are equivalent to bonds and atoms in molecules. Furthermore, graph theory enables the construction of tools that are very useful for a deeper understanding of chemical and physicochemical properties of molecules.

In the present report, the most important point is the concept of canonical structures and advantages due to making use of them. It is well known [9,10] that in many cases of π -electron systems the number of canonical structures, K , is related to the stability of the system in question. In organic chemistry, a given canonical structure is often considered as dominant and responsible for some chemical of physicochemical properties [11]. On the other hand, valence bond (VB) theory [12], natural resonance theory (NRT) [13], Hückel–Lewis projection method (HL-P) [14], electron localization function (ELF)

Pure Appl. Chem.* **84, 861–1112 (2012). A collection of invited papers based on presentations at the 14th International Symposium on Novel Aromatic Compounds (ISNA-14), Eugene, OR, USA, 24–29 July 2011.

[‡]Corresponding author: Fax: (+48) 22 8222892; E-mail: chamis@chem.uw.edu.pl

analysis [15], as well as empirical approaches [9,16] enable the quantitative estimate of the contributions of particular canonical structures in the description of a given molecular system. In this paper, we intend to present ways in which the concept of canonical structure may provide a deeper understanding of properties of given π -electron systems, in particular of benzenoid hydrocarbons.

ADJACENCY MATRIX

Any chemical structure may be represented by adjacency matrix **A**, which is illustrated as an example for naphthalene molecule in Fig. 1.

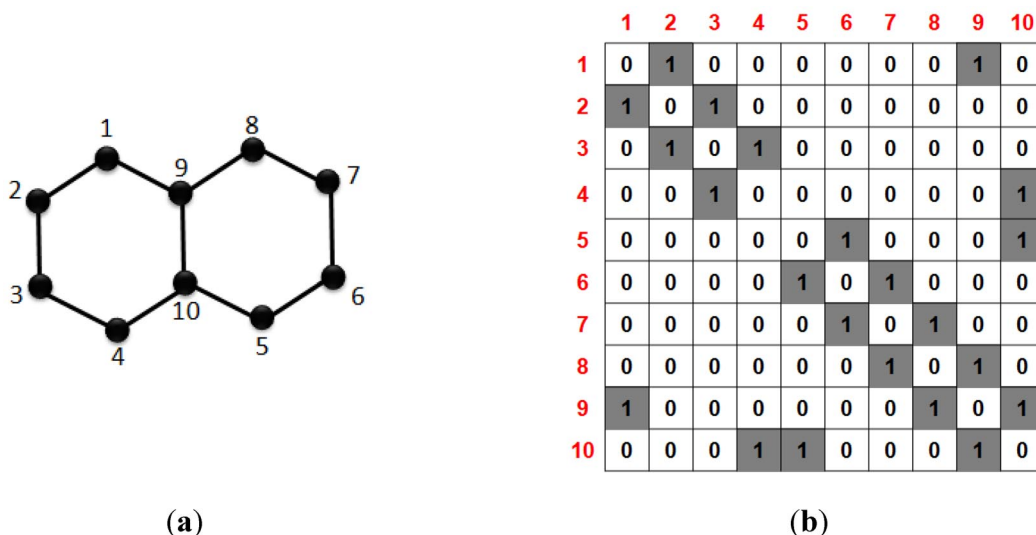


Fig. 1 (a) Naphthalene molecule with labeling of vertices. (b) Adjacency matrix for the molecule.

It is well known that the term $K = \sqrt{|\det \mathbf{A}|}$ allows the number of possible canonical structures K to be found, for any benzenoid system [10]. It has also been shown [17] that $\ln K$ strongly correlates with resonance energy (RE). By analogy with the Boltzmann definition of entropy [18,19], which takes into account the number of possible microstates corresponding to the macrostate of a system, a similar quantity was defined as $S = \ln K$ [18], which relates the number of canonical structures, i.e., the number of possible virtual states corresponding to the state of a benzenoid system. The S -values correlate well to the aromatic stabilization energy (ASE) [21], estimated with the use of ab initio optimized data by quantum chemical methods for 30 benzenoid hydrocarbons [20,22]. This relation is shown in Fig. 2.

When the adjacency matrix **A** is transferred into its inverse matrix \mathbf{A}^{-1} , then the obtained matrix elements represent Pauling π -bond orders. This is illustrated in Fig. 3.

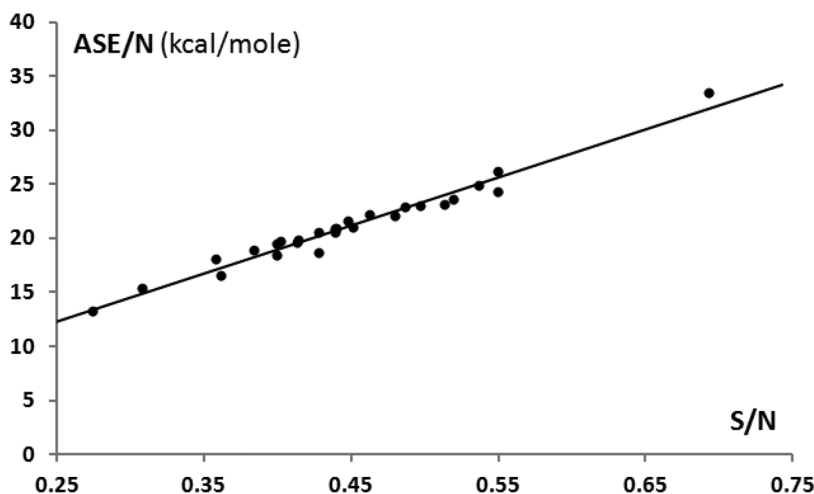


Fig. 2 Correlation between intensive values (calculated per ring) of ASE and $S = \ln K$ for 30 benzenoid hydrocarbons (correlation coefficient $R = 0.984$). N stands for number of six-membered rings.

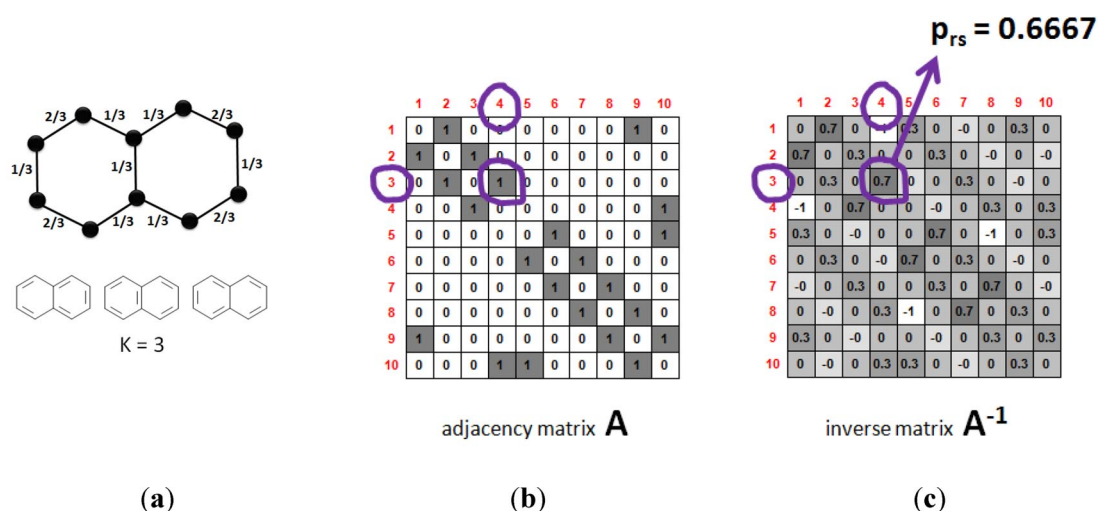


Fig. 3 Three canonical structures for naphthalene (a), adjacency matrix \mathbf{A} (b), and the Pauling π -inverse matrix \mathbf{A}^{-1} (c).

Consider now changed adjacency matrix in which only double bonds of a given canonical structure are taken into account as shown for benzene in Fig. 4. These kinds of matrices, named as the Kekulé matrices, labeled \mathbf{K} [23], have a particular property: the squared root of its determinant is equal to one, independently of the benzenoid system considered. The \mathbf{K} matrix can be obtained from the \mathbf{A} matrix by subtracting 1 from elements a_{pq} that represent single bonds in the Kekulé structure.

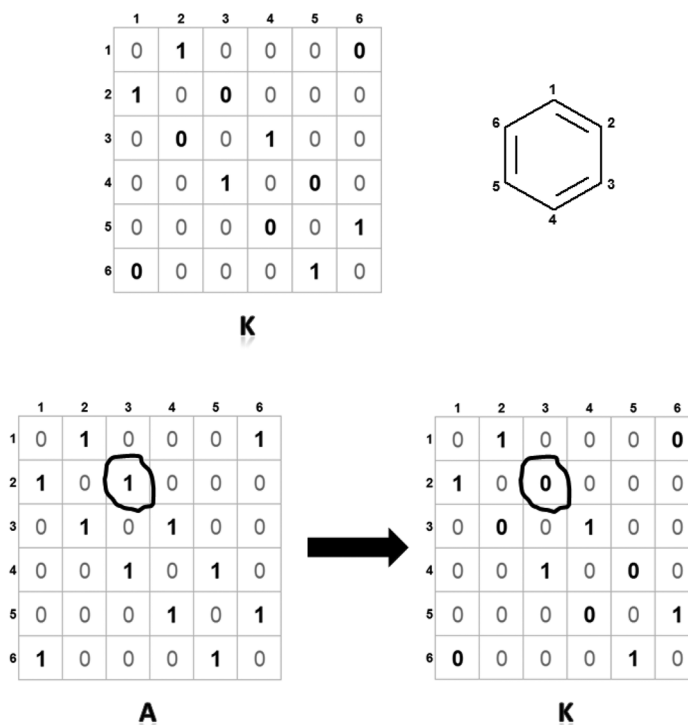


Fig. 4 The way of obtaining the **K** matrix from the **A** matrix for benzene.

The **K** matrix represents localized system obtained from the molecule described by matrix **A** [24]. Note that for this localized system $\ln K = 0$. This is a limit case of localization of an aromatic system also in the meaning of stabilization energy. Therefore, we may view **A** and **K** as representing two boundary cases for a molecule (benzene).

$$\ln \sqrt{|\det \mathbf{A}|} \sim RE \quad (1)$$

$$\ln \sqrt{|\det \mathbf{K}|} = 0 \quad (2)$$

Consider now a way in which we can pass from the adjacency matrix **A** to the Kekulé matrix **K**. We may consider that **A** and **K** are the boundary cases of a more general matrix **A**(ϵ), in which from elements a_{pq} that represent single bonds we subtract a value $\epsilon \in \langle 0,1 \rangle$ which represents a magnitude of the perturbation. Such a perturbation may be identified with the influence of external factor on the π -electron localization in the bond. This is exemplified for benzene in Fig. 5. When ϵ is equal to 1, then **A** \rightarrow **K**. Matrices of **A**(ϵ) type are named perturbation matrices [23]. **A**($\epsilon = 1$) and **A**($\epsilon = 0$) correspond to the localized and delocalized structures, respectively.

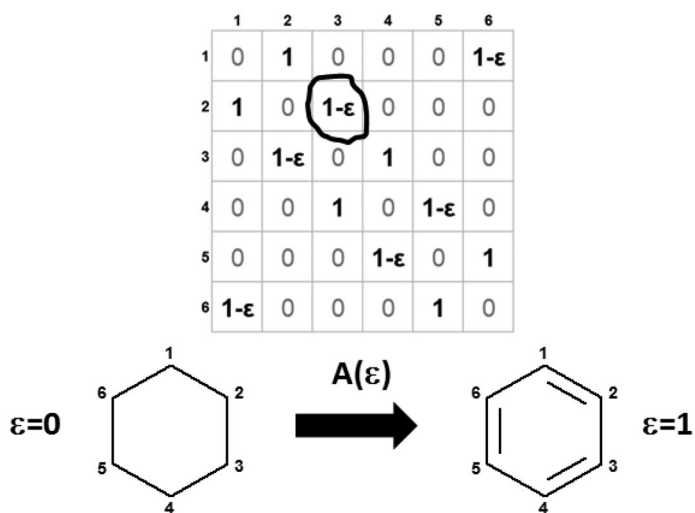


Fig. 5 The Kekulé matrix for the one canonical structure of benzene.

For each $\det A(\epsilon)$, the Kekulé polynomial $P(\epsilon)$ may be obtained, as it is shown for one of the canonical structures for benzene in Fig. 6.

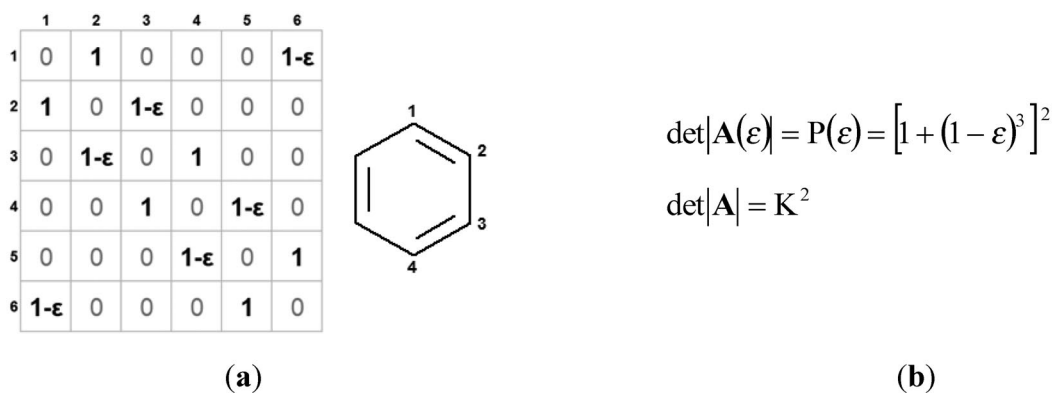


Fig. 6 The $A(\epsilon)$ matrix (a) and Kekulé polynomial $P(\epsilon)$ (b) for the one structure of benzene.

Figure 7 presents a dependence of value of the determinant of a given canonical structure of benzene on the strength of perturbation, ϵ .

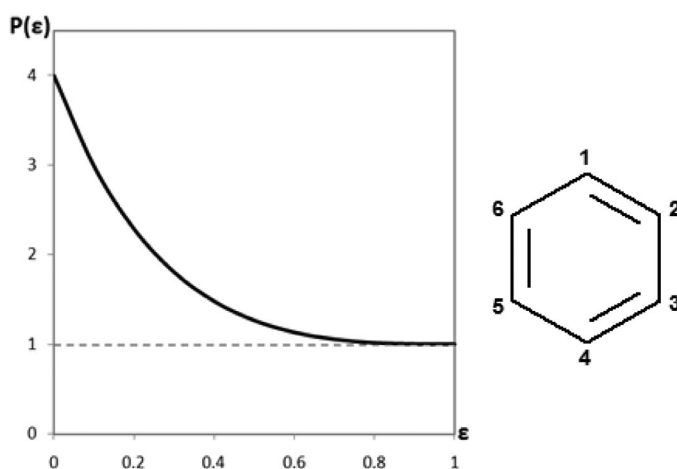
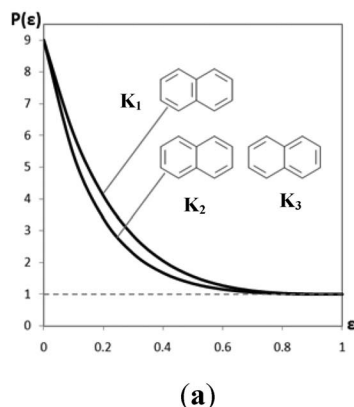


Fig. 7 The dependence of $P(\varepsilon)$ on the strength of perturbation ε . Reprinted with permission from ref. [23]. Copyright © 2011 Royal Society of Chemistry.

For more complex molecules, the number of canonical structures increases. As might be expected for symmetry-independent canonical structures, the polynomials are different. What is more, the dependence of $P(\varepsilon)$ on ε is also different for each symmetrically independent canonical structures. This point is exemplified in Fig. 8 by naphthalene and its canonical structures.



$$K_1: \quad \det|\mathbf{A}(\varepsilon)| = P(\varepsilon) = [1 + 2(1 - \varepsilon)^3]^2$$

$$K_{2,3}: \quad \det|\mathbf{A}(\varepsilon)| = P(\varepsilon) = [1 + (1 - \varepsilon)^3 + (1 - \varepsilon)^5]^2$$

(b)

Fig. 8 The dependence of $P(\varepsilon)$ on the magnitude of perturbation ε for two symmetrically independent structures of naphthalene (a) and Kekulé polynomial $P(\varepsilon)$ —the upper and lower polynomial refers to K_1 and K_2 (or K_3) canonical structure, respectively (b). Reprinted with permission from ref. [23]. Copyright © 2011 Royal Society of Chemistry.

While looking at curves in Fig. 8, we note the dependences $P(\varepsilon)$ on ε differ in their shape. The steeper curve corresponds to the symmetrical canonical structure, which according to empirical estimation of weights of canonical structure by the HOSE model [16] contributes in 48.4 %. The other two canonical structures (the remaining line) contribute to 25.8 % each. Importantly, the derivatives of $P(\varepsilon)$ at $\varepsilon = 0$ for particular canonical structures in form of eq. 3 are strongly correlated with the canonical structure weights estimated with use of the HOSE model [16]. The dependence for benzenoid hydrocarbons is presented in Fig. 9.

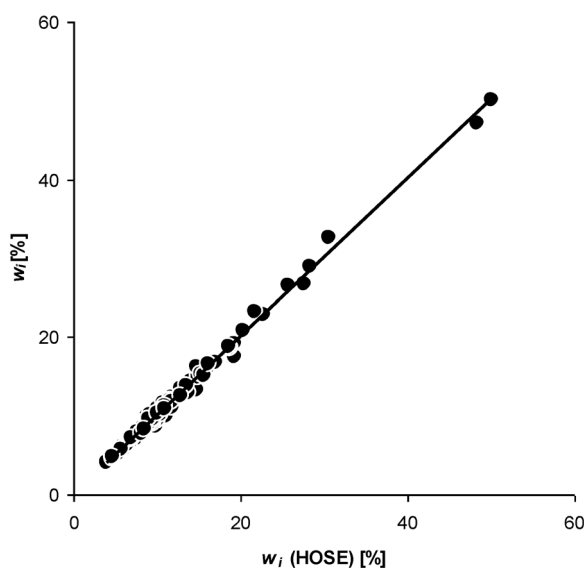


Fig. 9 Dependence between the weights of the canonical structures obtained from the polynomial $P(\varepsilon)$ and calculated according to the HOSE model [$w_i(\text{HOSE})$]. Correlation coefficient $R = 0.997$ (150 points corresponding to canonical structures of 18 benzenoid hydrocarbons) [23].

$$w_i = \frac{\left(\frac{dP_i(\varepsilon=0)}{d\varepsilon}\right)^{-2}}{\sum_{i=1}^k \left(\frac{dP_i(\varepsilon=0)}{d\varepsilon}\right)^{-2}} \cdot 100\% \quad (3)$$

It is important to note here that the HOSE model is based on geometry (bond lengths), whereas the derivative method is based on non-metric graph-topological approach.

THE HÜCKEL RULE

Why and how does the Hückel rule work? Analysis of Kekulé polynomials for monocyclic π -electron hydrocarbons (Fig. 10) brings an answer for this question. Table 1 presents the Kekulé polynomials for

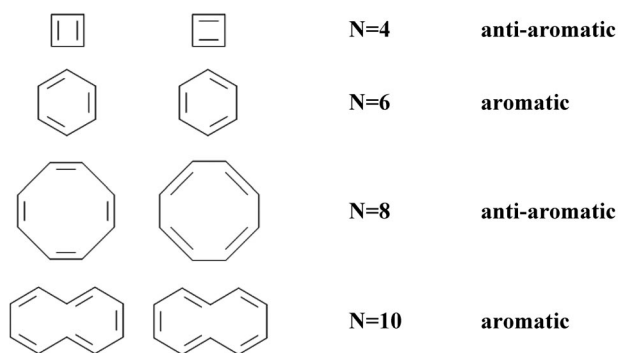


Fig. 10 Aromatic and anti-aromatic monocyclic conjugated systems. N denotes number of π -electrons.

monocycles, whereas Fig. 11 shows their dependences of the extent of perturbation parameter ε . Note that the exponent n of the $(1 - \varepsilon)^n$ is equal to half of the number of π -electrons $N/2$ in a given ring, or more generally in a given conjugated cycle.

Table 1 Kekulé polynomials for the annulenes.

[4]annulene (cyclobutadiene)	$P(\varepsilon) = [1 - (1 - \varepsilon)^2]^2$
[6]annulene (benzene)	$P(\varepsilon) = [1 + (1 - \varepsilon)^3]^2$
[8]annulene	$P(\varepsilon) = [1 - (1 - \varepsilon)^4]^2$
[10]annulene	$P(\varepsilon) = [1 + (1 - \varepsilon)^5]^2$
[12]annulene	$P(\varepsilon) = [1 - (1 - \varepsilon)^6]^2$
[14]annulene	$P(\varepsilon) = [1 + (1 - \varepsilon)^7]^2$
[N]annulene	$P(\varepsilon) = [1 - (-1 - \varepsilon)^{N/2}(1 - \varepsilon)^{N/2}]^2$

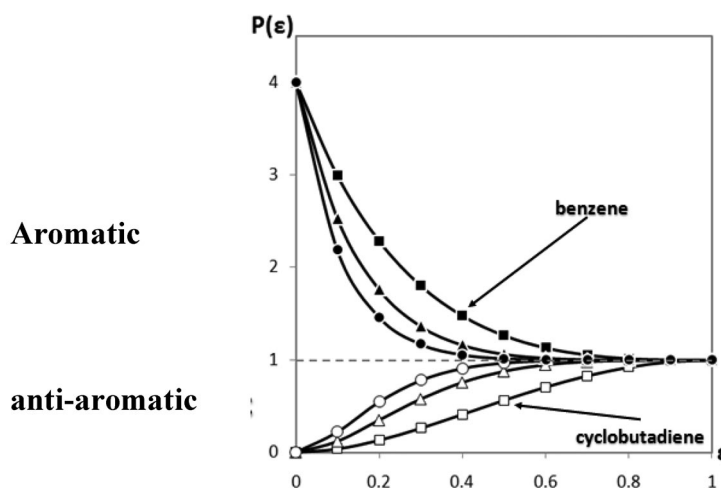


Fig. 11 Dependences of $P(\varepsilon)$ on the extent of perturbation ε for aromatic and anti-aromatic annulenes. \square stands for [4]annulene (cyclobutadiene); \blacksquare stands for [6]annulene (benzene); \triangle stands for [8]annulene; \blacktriangle stands for [10]annulene; \circ stands for [12]annulene; \bullet stands for [14]annulene. Reprinted with permission from ref. [23]. Copyright © 2011 Royal Society of Chemistry.

If the areas under the curves in Fig. 11 are calculated in a way that the formula $S = \ln K$ is taken instead of K , the area under the curve represented by $P(\varepsilon)$

$$S/N = \frac{1}{N} \ln \left[\int_0^1 P(\varepsilon) d\varepsilon \right] \quad (4)$$

then for $4N + 2$ cycles the positive values, whereas for $4N$ cycles the negative ones are obtained. The scatter plot of S/N vs. number of π -electrons shows a characteristic zigzag shape (see Fig. 12), similar to those published earlier by using various quantum-chemical approaches [25–28].

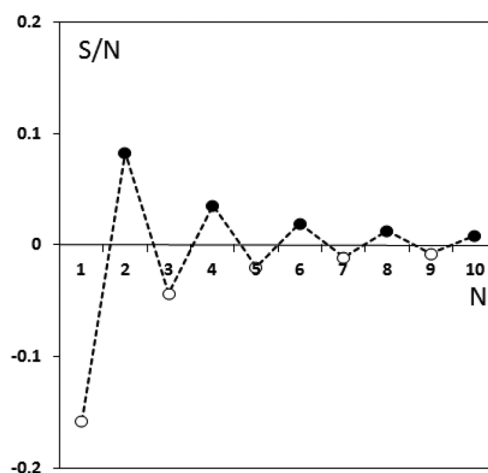


Fig. 12 S/N values calculated for $4N + 2$ and $4N$ annulenes.

The Hückel rule works in principle only for monocyclic systems, however, some extensions of its applications seem to be very interesting. Consider benzocyclobutadiene and its three canonical structures as an example (Table 2). In two of three canonical structures of benzocyclobutadiene a formal cyclobutadiene unit can be distinguished, the cycle known as being destabilizing [22,29]. In polynomials, both negative and positive contributions of $(1 - \epsilon)$ terms are present. Clearly, the positive contribution is related to $4N + 2$ conjugated cycles present in a given canonical structure, whereas the negative ones refer to the $4N$ conjugated cycles.

Table 2 Canonical structures of benzocyclobutadiene and the corresponding Kekulé polynomials.

	$[1 + (1 - \epsilon)^3 - (1 - \epsilon)^4]^2$
	$[1 - (1 - \epsilon)^2 + (1 - \epsilon)^3]^2$
	$[1 - (1 - \epsilon)^2 - (1 - \epsilon)^4]^2$

The dependences of $P(\epsilon)$ on the magnitude of perturbation ϵ for all three canonical structures are shown in Fig. 13.

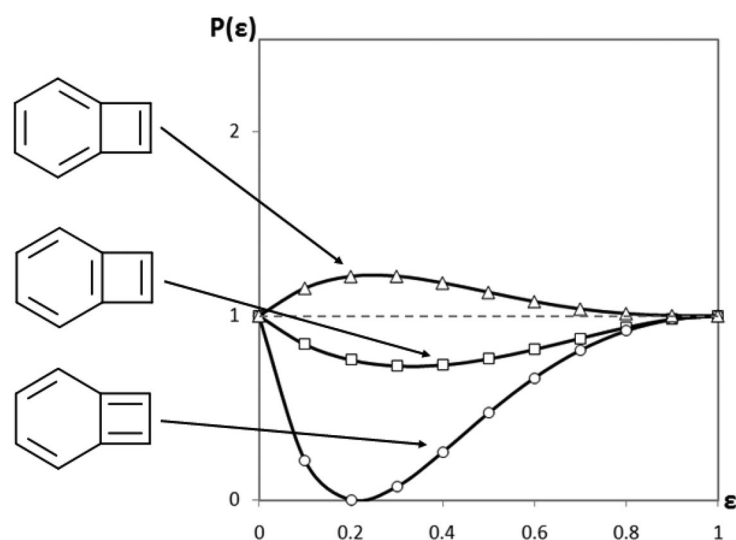


Fig. 13 Dependencies of $P(\epsilon)$ on ϵ for three structures of benzocyclobutadiene. Reprinted with permission from ref. [23]. Copyright © 2011 Royal Society of Chemistry.

Benzocyclobutadiene is composed of one stabilizing canonical structure and two destabilizing ones. This is not only reflected in the dependence of $P(\epsilon)$ on ϵ , but also in the geometry of the system (both based on calculations and experiment, see Fig. 14). Clearly, the stabilizing canonical structure dominates.

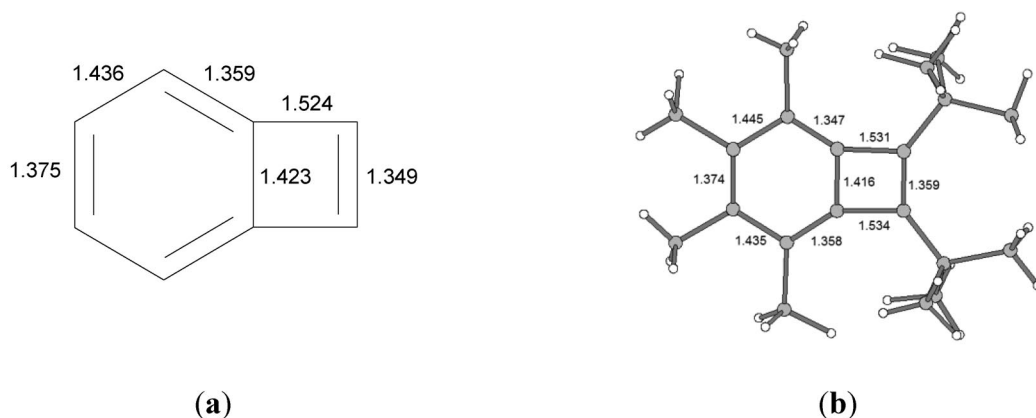


Fig. 14 The structures of benzocyclobutadiene (a) optimized at B3LYP/6-311G** level of theory [36] and (b) the experimental geometry of benzocyclobutadiene derivative [37]. The bond lengths indicate contribution of one canonical structure.

The Hückel rule and its consequences for more complex systems are also nicely illustrated by experimental studies of benz[*c*]octalen. The molecule is composed of conjugated cycles containing both $4N$ and $4N + 2$ π -electrons. As a matter of fact, the compound exists in solution as a mixture of two types of isomers, say A and B (see Fig. 15 and Table 3) whereas in crystalline state, the isomer A is preferred [30,31]. The total energy difference between A and B calculated at B3LYP/6-311G** level of theory [30] equals to ca. 1.5 kcal/mol, indicating the A form is more stable (Fig. 16). Explanation of this fact can be easily given by application of the methodology presented in this paper.

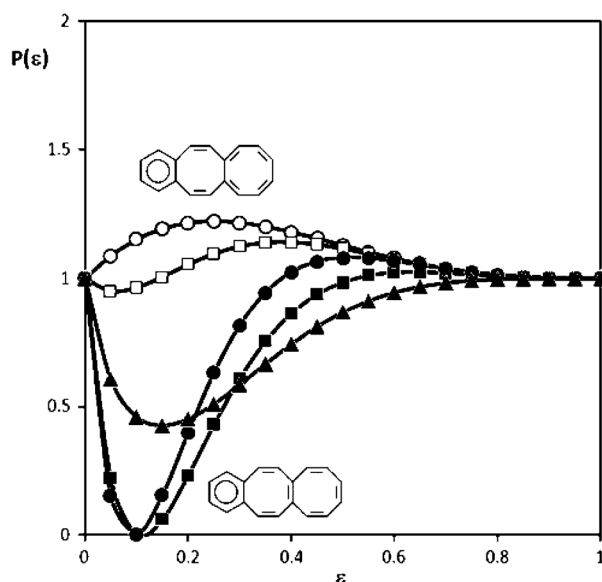


Fig. 15 The dependence of Kekulé polynomials on the magnitude of perturbation ε for five structures k_1 (\circ), k_2 (\square), k_3 (\blacksquare), k_4 (\bullet), and k_5 (\blacktriangle) of benz[*c*]octalene (for enumeration, see Table 2). Reprinted with permission from ref. [23]. Copyright © 2011 Royal Society of Chemistry.

Table 3 Canonical structures of benz[*c*]octalene and the corresponding Kekulé polynomials.

k_1		$P_1(\varepsilon) = [1 + (1 - \varepsilon)^3 - (1 - \varepsilon)^4 + (1 - \varepsilon)^7 - (1 - \varepsilon)^7]^2$
k_2	 (a)	$P_2(\varepsilon) = [1 + (1 - \varepsilon)^3 - (1 - \varepsilon)^4 - (1 - \varepsilon)^7 + (1 - \varepsilon)^9]^2$
k_3		$P_3(\varepsilon) = [1 + (1 - \varepsilon)^3 - 2(1 - \varepsilon)^4 - (1 - \varepsilon)^7]^2$
k_4	 (b)	$P_4(\varepsilon) = [1 + (1 - \varepsilon)^3 - (1 - \varepsilon)^4 - (1 - \varepsilon)^6 - (1 - \varepsilon)^7]^2$
k_5		$P_5(\varepsilon) = [1 + (1 - \varepsilon)^4 - (1 - \varepsilon)^6 + (1 - \varepsilon)^7 + (1 - \varepsilon)^9]^2$

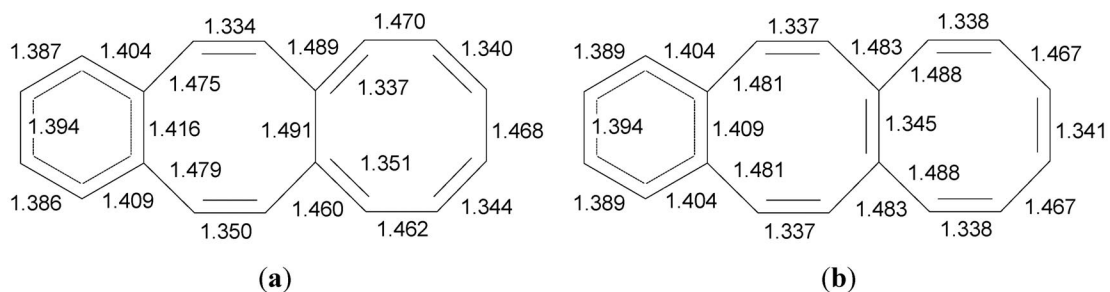


Fig. 16 The calculated geometries of two forms of benz[*c*]octalene.

Table 3 presents five possible canonical structures of benz[*c*]octalene and the corresponding Kekulé polynomials $P_i(\epsilon)$. It is seen from Fig. 15 that canonical structures for A (k_1 and k_2) are stabilizing, whereas those for B are destabilizing (k_3 , k_4 , and k_5). Thus, in isotropic situation in solution benz[*c*]octalene may exist in two different electronic states, i.e., as isomers. In the solid state, such possibility is reduced.

THE CLAR CLASSIFICATION

Clar's classification [32,33] is related to differences in the π -electron structure of individual rings of benzenoid hydrocarbons. Triphenylene, phenanthrene, and anthracene (Fig. 17) are typical examples. The classification distinguishes particular types of rings, as follows:

- aromatic sextets such as, e.g., benzene or three terminal rings in triphenylene;
- migrating sextets such as, e.g., rings in naphthalene or anthracene;
- empty rings such as, e.g., the central ring of triphenylene or perylene; and
- rings with localized double bonds such as, e.g., the central ring in phenanthrene.

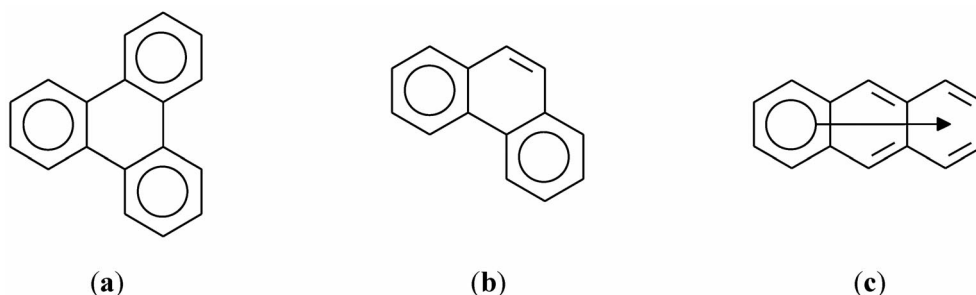


Fig. 17 The types of Clar's rings.

Let us consider all canonical structure of phenanthrene. They are presented in Table 4.

In the first structure of phenanthrene, k_1 , we can distinguish four conjugated cycles. The 6-membered cycle located in the center of the molecule is described by the term $+(1 - \epsilon)^3$. The remaining terms of the polynomials $+2(1 - \epsilon)^5$ and $(1 - \epsilon)^7$ indicate the existence of two 10-membered cycles and one 14-membered cycle. All of them are found in Table 4.

For the remaining canonical structures, k_2 – k_5 , there is an additional, stabilizing term $+(1 - \epsilon)^6$. It could be supposed that there is a 12-membered cycle, which however does not exist in these canonical structures. The only explanation may be that this positive contributor comes from two distinct benzene circuits, which coexist and stabilize the system. This situation is referred to as one of the Clar structures of phenanthrene in which we can distinguish two coexisting sextets (Fig. 17). Note that the term $+(1 - \epsilon)^6$ is a product of two terms $(1 - \epsilon)^3$, i.e., $(1 - \epsilon)^3(1 - \epsilon)^3$, which represent two 6-membered cycles. In a similar way, one of the Clar structures of triphenylene (with the so-called empty central ring, Fig. 17) may be illustrated. In this case, the perturbation polynomial contains the term $(1 - \epsilon)^9$, which can be viewed as a product of three $(1 - \epsilon)^3$ terms.

Table 4 Decomposition of symmetrically independent canonical structures of phenanthrene k_1 , k_2 , $k_3 = k_4$ and k_5 into conjugated circuits. Reprinted with permission from ref. [23]. Copyright © 2011 Royal Society of Chemistry.

			
k_1	$+(1 - \varepsilon)^3$	$+(1 - \varepsilon)^5$	$+(1 - \varepsilon)^5$
			$+(1 - \varepsilon)^7$
	$P_1(\varepsilon) = [1 + (1 - \varepsilon)^3 + 2(1 - \varepsilon)^5 + (1 - \varepsilon)^7]^2$		
			
k_2	$+(1 - \varepsilon)^3$	$+(1 - \varepsilon)^3$	$+(1 - \varepsilon)^3$
			$+(1 - \varepsilon)^6$
	$P_2(\varepsilon) = [1 + 3(1 - \varepsilon)^3 + (1 - \varepsilon)^6]^2$		
			
$k_3 = k_4$	$+(1 - \varepsilon)^3$	$+(1 - \varepsilon)^5$	$+(1 - \varepsilon)^3$
			$+(1 - \varepsilon)^6$
	$P_3(\varepsilon) = [1 + 2(1 - \varepsilon)^3 + (1 - \varepsilon)^5 + (1 - \varepsilon)^6]^2 = P_4(\varepsilon)$		
			
k_5	$+(1 - \varepsilon)^3$	$+(1 - \varepsilon)^3$	$+(1 - \varepsilon)^7$
			$+(1 - \varepsilon)^6$
	$P_5(\varepsilon)[1 + 2(1 - \varepsilon)^3 + (1 - \varepsilon)^6 + (1 - \varepsilon)^7]^2$		

It is important to note that this approach allows one to distinguish all kinds of conjugated cycles which contribute to overall stability. In the case of coronene (Fig. 18) in one of canonical structures, a term $(1 - \varepsilon)^{12}$ appears, indicating the coexistence of the central ring sextet with supersextet with 18 π -electrons, which was postulated by Hosoya two decades ago [34].

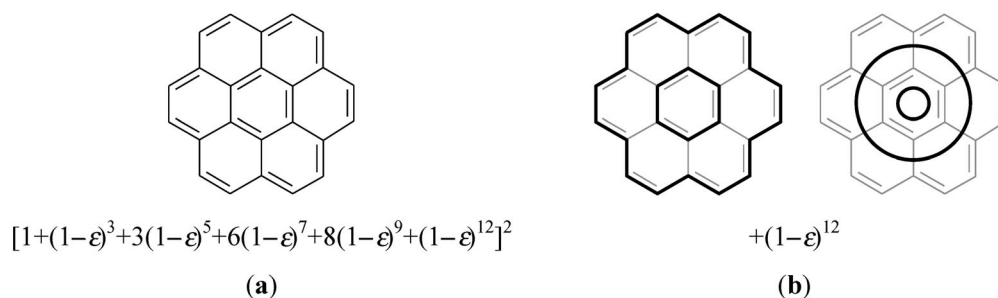
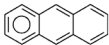
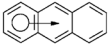
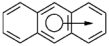
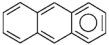


Fig. 18 (a) One of the canonical structures of coronene with its Kekulé polynomial. (b) The two coexisting 6- and 18-membered circuits with the appropriate polynomial term. On the right are the Clar sextet circle and the Hosoya super sextet. Reprinted with permission from ref. [23]. Copyright © 2011 Royal Society of Chemistry.

In the case of migrating sextets, we can see the sextet may be attributed to only one ring [here is only one term $(1 - \varepsilon)^3$] as shown in Table 5.

Table 5 Clar structures of anthracene with Kekulé polynomial terms associated with a sextet or migrating sextet and Kekulé polynomial $P(\varepsilon)$ for a given structure. Reprinted with permission from ref. [23]. Copyright © 2011 Royal Society of Chemistry.

Canonical structure	$P_i(\varepsilon)$
k_1  $+(1 + \varepsilon)^3$	$[1 + (1 - \varepsilon)^3 + (1 - \varepsilon)^5 + (1 - \varepsilon)^7]^2$
k_2  $+(1 + \varepsilon)^3 + (1 + \varepsilon)^3$	$[1 + 2(1 - \varepsilon)^3 + (1 - \varepsilon)^5]^2$
k_3  $+(1 + \varepsilon)^3 + (1 + \varepsilon)^3$	$[1 + 2(1 - \varepsilon)^3 + (1 - \varepsilon)^5]^2$
k_4  $+(1 + \varepsilon)^3$	$[1 + (1 - \varepsilon)^3 + (1 - \varepsilon)^5 + (1 - \varepsilon)^7]^2$

MAGNETIC PROPERTIES OF BENZENOID HYDROCARBONS

Consider nine canonical structures of benz[*a*]pyrene (Fig. 19).

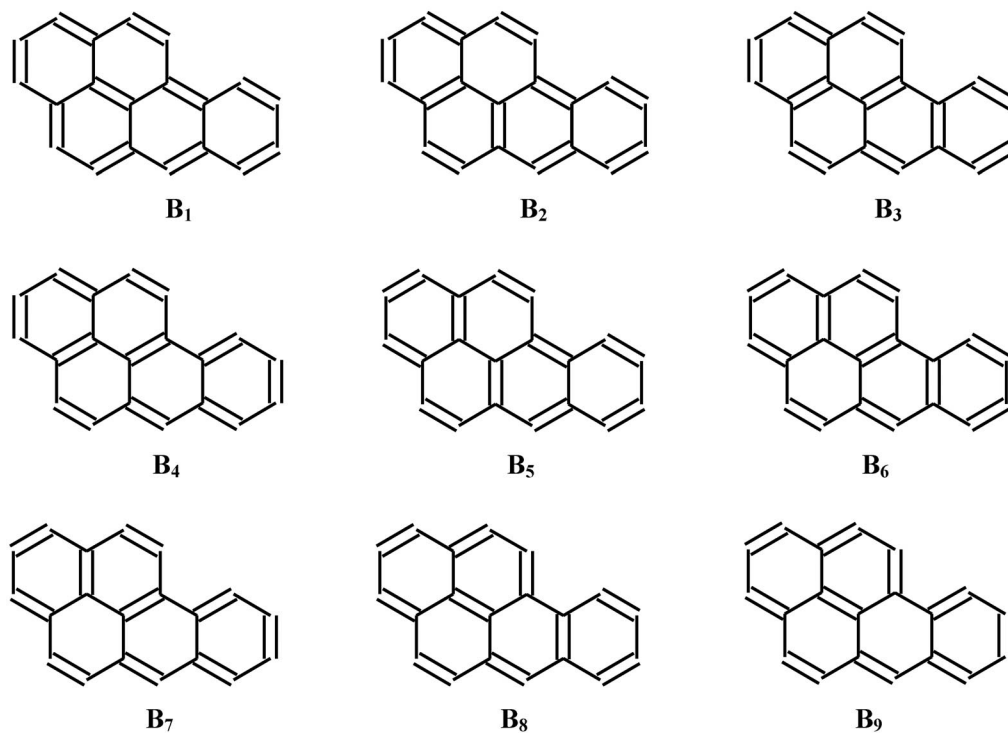


Fig. 19 Canonical structures for benz[*a*]pyrene. Reprinted with permission from ref. [38]. Copyright © 2011 Royal Society of Chemistry.

We can define an operation in which we obtain so-called symmetric differences between two given canonical structures (Fig. 20), which are represented in this case by two conjugated cycles.

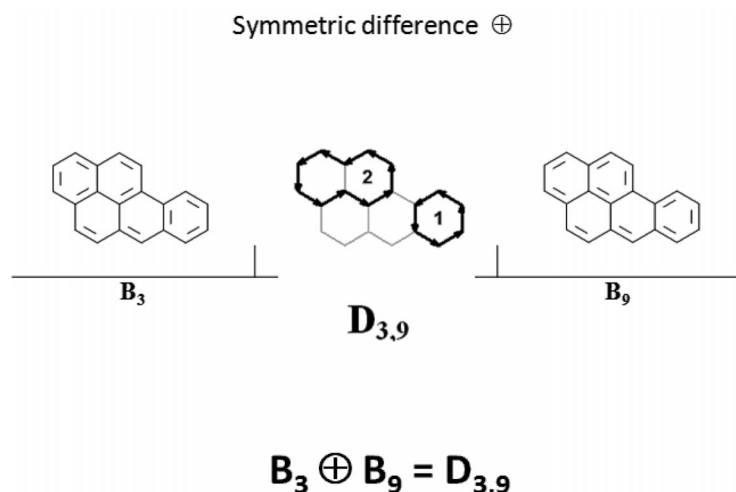


Fig. 20 Symmetric difference between two canonical structures of benz[*a*]pyrene B_3 and B_9 gives circuit structure $D_{3,9}$.

The obtained cycles may be applied to find representation of partial ring currents if the molecule is exposed to the perpendicular magnetic field. The arrows indicate the direction of the induced ring current. Symmetric differences of all possible pairs of canonical structures lead to all partial contributors to the overall induced ring currents, the so-called circuit structures, as shown in Fig. 21.

If we superimpose them [37], then a map with weights representing the intensity of ring current for each given bond is obtained. This map is in excellent agreement with the calculated map of induced ring current within an ipsocentric approach. This is true not only for benz[*a*]pyrene (discussed here), but also for other benzenoids [37] (Fig. 22).

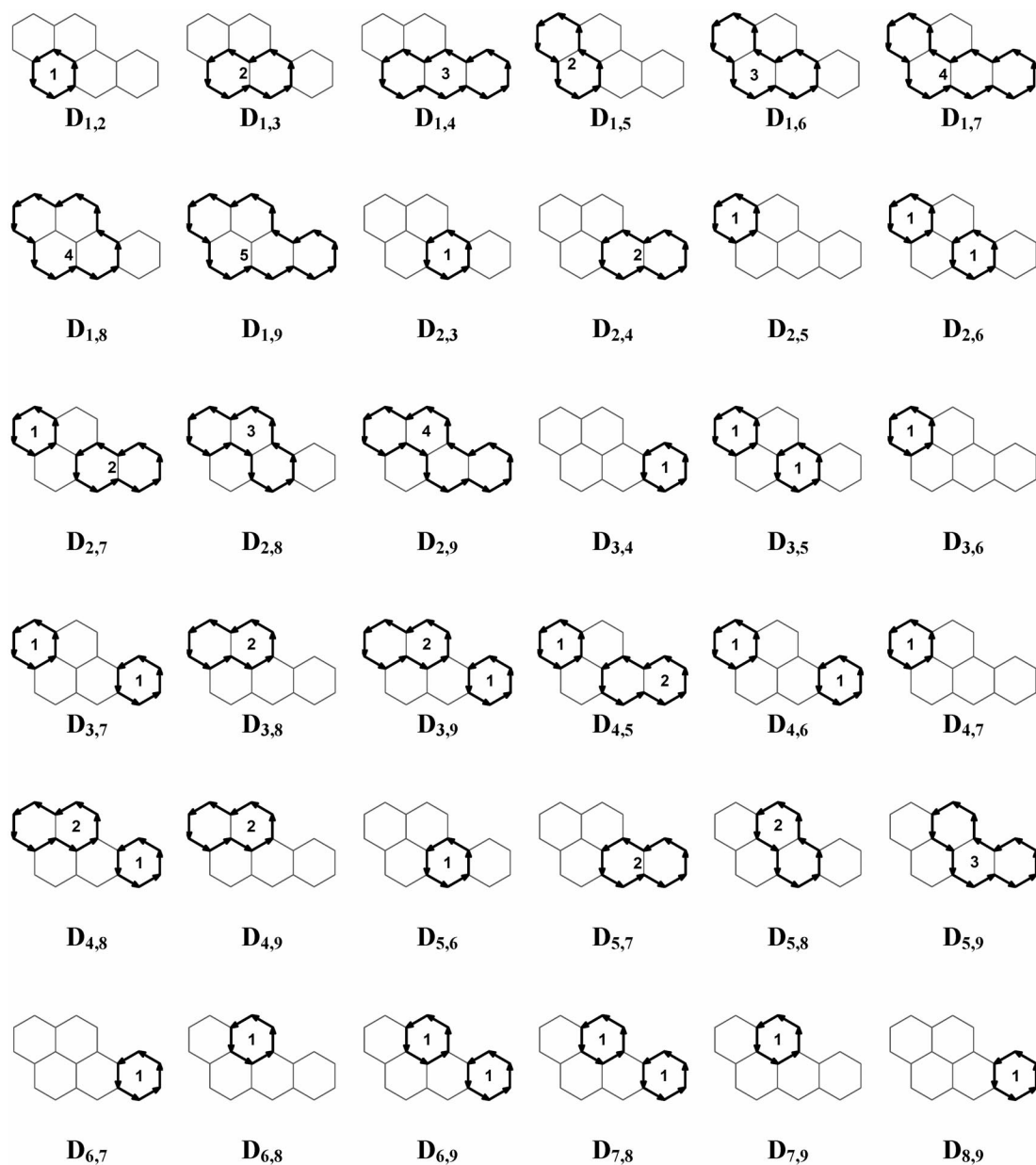


Fig. 21 All possible circuit structures for benz[a]pyrene. Reprinted with permission from ref. [37]. Copyright © 2011 Royal Society of Chemistry.

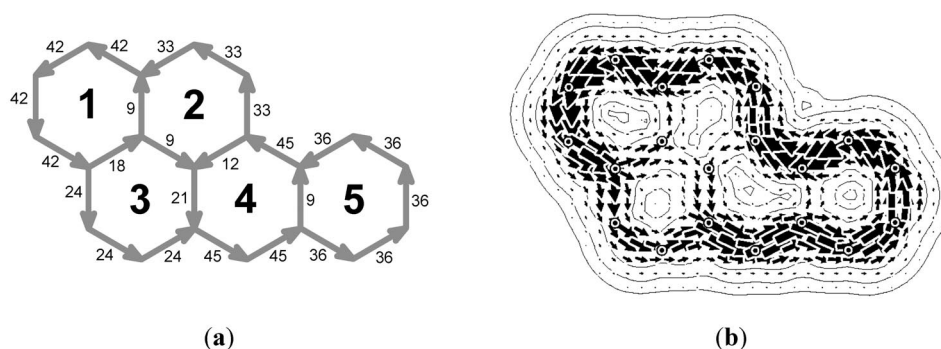


Fig. 22 Diagram obtained by superposing all circuit structures (a) and ipsocentric approach map of induced ring currents for benz[*a*]pyrene (b). Reprinted with permission from ref. [37]. Copyright © 2011 Royal Society of Chemistry. The numbers denote the contribution weights representing ring current intensities.

QUANTIFICATION OF MAGNETIC PROPERTIES OF BENZENOID HYDROCARBONS

Superimposed directed graph structures (Fig. 22) can be decomposed into contributions owing to individual rings. This is shown in Fig. 23 [37].

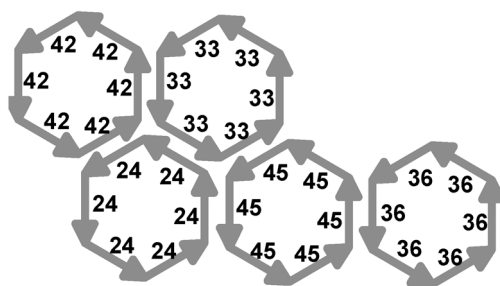


Fig. 23 Decomposition into elementary circuits. Reprinted with permission from ref. [37]. Copyright © 2011 Royal Society of Chemistry. The numbers denote the contribution weights representing ring current intensities.

Based on this approach, we define global magnetic characteristics (GMC) by the following formula:

$$\text{GMC} = \frac{\sum_i^n N_i}{\frac{1}{2}(K-1)K} \quad (5)$$

where N_i is a contribution of the i -th ring to the overall induced ring current and K is the number of canonical structures, whereas n is the number of six-membered rings. The dependence of normalized GMC/n^2 on exaltation of magnetic susceptibility $\Delta\lambda/n^2$ is presented in Fig. 24.

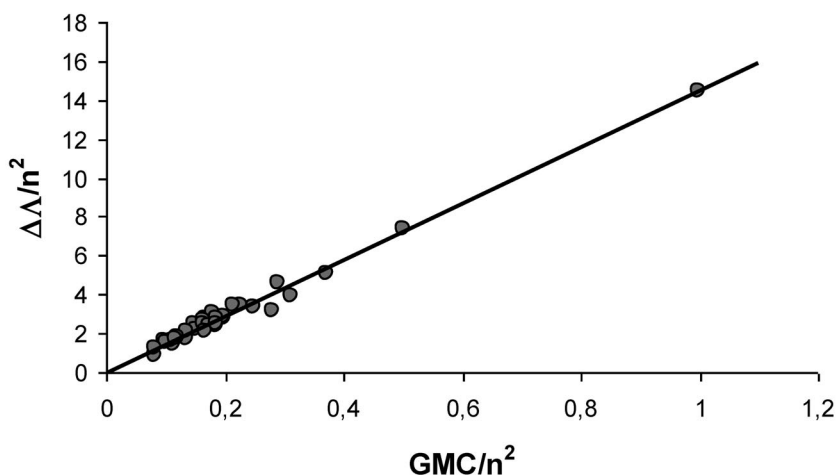


Fig. 24 Correlation between exaltation of magnetic susceptibility $\Delta\Lambda/n^2$ and GMC/n^2 (correlation coefficient $R = 0.992$). Reprinted with permission from ref. [37]. Copyright © 2011 Royal Society of Chemistry.

The approach also allows the quantification of local magnetic properties, as, e.g., Schleyer's nucleus-independent chemical shift (NICS) [35]. For a given ring, the local magnetic characteristics (LMC) are defined by the following formula:

$$LMC = \frac{\sum_{i=1}^b \delta_i w_i}{b \cdot \frac{1}{2}(K-1)K} \quad (6)$$

where w_i is the weight of the induced ring current for i -th bond, δ_i is equal to +1 for the anti-clockwise direction of an arrow in a given ring, and -1 for the clockwise direction, K is the number of canonical structures, and $b = 6$ for six-membered rings. Figure 25 presents a scatterplot of NICS(1) values against LMC for 129 rings of 34 benzenoid hydrocarbons.

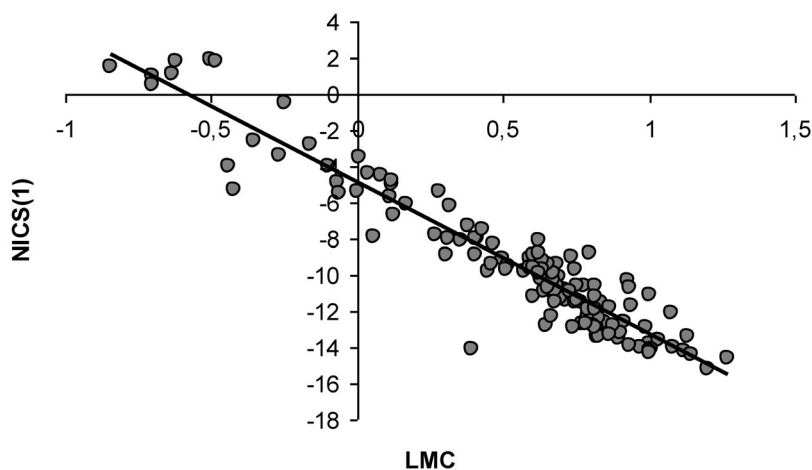


Fig. 25 Dependence of NICS(1) vs. LMC values calculated for 129 rings of 34 benzenoid hydrocarbons (correlation coefficient $R = 0.949$). Reprinted with permission from ref. [37]. Copyright © 2011 Royal Society of Chemistry.

CONCLUSIONS

The approach based on graph theory and topological properties of the molecules of π -electron hydrocarbons allowed us to derive, but also to extend, fundamental rules of aromaticity, such as the Hückel rule and the Clar classification. The perturbation-like approach based on the adjacency matrix and its transformation into a form describing the canonical structures allows their gradation and shows which of them are stabilizing or destabilizing. Graph theory is also efficient in interpretation of ring current formation in molecules when exposed to an external magnetic field and allows us to construct topology-derived characteristics such as GMC and LMC. The estimation of RE-like characteristics is also possible.

ACKNOWLEDGMENTS

We gratefully acknowledge financial support from Grant 501/64-BST-160106. D. K. S. acknowledges the Interdisciplinary Centre for Mathematical and Computational Modelling (Warsaw, Poland) for computational facilities. This paper is dedicated to our friend Prof. Wojciech Grochala (University of Warsaw) on the occasion of his 40th birthday.

REFERENCES

1. R. J. Wilson. *Introduction to Graph Theory*, Longman, Essex (1996).
2. I. Gutman, M. Milun, N. Trinajstić. *J. Am. Chem. Soc.* **99**, 1692 (1977).
3. R. Chauvin, C. Lepetit, V. Maraval, L. Leroyer. *Pure Appl. Chem.* **82**, 769 (2010).
4. M. Randić. *J. Chem. Inf. Comput. Sci.* **44**, 365 (2004).
5. N. Biggs, E. Lloyd, R. Wilson. *Graph Theory*, Oxford University Press, Oxford (1986).
6. M. V. Diudea, M. S. Florescu, P. V. Khadikar. *Molecular Topology and Its Applications*, Eficon Press, Bucharest (2006).
7. M. I. Monastyrsky. *Topology in Molecular Biology (Biological and Medical Physics, Biomedical Engineering)*, Springer, Berlin (2007).
8. A. T. Balaban, J. Devillers. *Topological Indices and Related Descriptors in QSAR and QSPAR*, CRC Press, Boca Raton (2000).
9. M. Randić. *Chem. Rev.* **103**, 3449 (2003).
10. N. Trinajstić. *Chemical Graph Theory*, CRC Press, London (1992).
11. M. B. Smith, J. March. *March's Advanced Organic Chemistry*, Wiley-Interscience, New York (2001).
12. A. Pross. *Theoretical and Physical Principles of Organic Reactivity*, John Wiley, New York (1995).
13. E. D. Glendening, F. Weinhold. *J. Comput. Chem.* **19**, 593 (1998).
14. Y. Carissan, D. Hagebaum-Reignier, N. Goudard, S. Humbel. *J. Phys. Chem. A* **112**, 13256 (2008).
15. C. Lepetit, B. Silvi, R. Chauvin. *J. Phys. Chem. A* **107**, 464 (2003).
16. T. M. Krygowski, R. Anulewicz, J. Kruszewski. *Acta Crystallogr., B* **39**, 732 (1983). The harmonic oscillator stabilization energy (HOSE) is defined as follows:

$$\text{HOSE}_i = 301.15 \cdot \left[\sum_{r=1}^{n_1} (R_r' - R_0^s)^2 \cdot k_r' + \sum_{r=1}^{n_2} (R_r'' - R_0^d)^2 \cdot k_r'' \right]$$

where R_r' and R_r'' stand for the bond lengths of a molecule; R_0^s and R_0^d stand for formal single and double bond in the i -th canonical structure, n_1 and n_2 are the numbers of the corresponding formal single and double bonds in the i -th canonical structure, respectively. k_r stands for force

constants. In the process of deformation, the n_1 bonds corresponding to the single bonds in the i -th canonical structure are lengthened, whereas the n_2 bonds corresponding to the double bonds in the i -th canonical structure are shortened, respectively. Each canonical structure may have a different HOSE value. The weight of the i -th canonical structure, w_i , in the description of geometry of the real molecule is inversely proportional to its destabilization energy (i.e., HOSE_{*i*}) the energy by which the i -th canonical structure is less stable than the real molecule:

$$w_i = \frac{[\text{HOSE}_i]^{-1}}{\sum_{i=1}^N [\text{HOSE}_i]^{-1}} \cdot 100\%$$

The summation runs over all structures.

17. R. Swinborn-Sheldrake, W. C. Herndon, I. Gutman. *Tetrahedron Lett.* **16**, 755 (1975).
18. S. G. Brush. *Statistical Physics and the Atomic Theory of Matter from Boyle and Newton to Landau and Onsager*, Princeton University Press, Princeton (1983).
19. P. M. E. Shutler, H. M. Cheah. *Eur. J. Phys.* **19**, 371 (1998).
20. A. Ciesielski, T. M. Krygowski, M. K. Cyrański, M. A. Dobrowolski, A. Balaban. *J. Chem. Inf. Model.* **49**, 369 (2009).
21. M. K. Cyrański. *Chem. Rev.* **105**, 3773 (2005).
22. P. George, M. Trachtman, C. W. Bock, A. M. Brett. *J. Chem. Soc., Perkin Trans. 2* 1222 (1976).
23. A. Ciesielski, T. M. Krygowski, M. K. Cyrański, A. Balaban. *Phys. Chem. Chem. Phys.* **13**, 3737 (2011).
24. J. -P. Malrieu, M. Gicquel, P. W. Fowler, C. Lepetit, J.-L. Heully, R. Chauvin. *J. Phys. Chem.* **112**, 13203 (2008).
25. M. J. S. Dewar, G. J. Gleicher. *J. Am. Chem. Soc.* **87**, 635 (1965).
26. H. P. Figeys. *Tetrahedron* **26**, 5225 (1970).
27. T. M. Krygowski. *Tetrahedron Lett.* **13**, 1311 (1972).
28. T. M. Krygowski, J. Kruszewski. *Bull. Acad. Polon. Sci.* **21**, 509 (1972).
29. Y. R. Mo, P. v. R. Schleyer. *Chem.—Eur. J.* **12**, 2009 (2006).
30. M. J. Frisch, G. W. Trucks, H. B. Schlegel, G. E. Scuseria, M. A. Robb, J. R. Cheeseman, J. A. Montgomery, T. Vreven, K. N. Kudin, J. C. Burant, J. M. Millam, S. S. Iyengar, J. Tomasi, V. Barone, B. Mennucci, M. Cossi, G. Scalmani, N. Rega, G. A. Petersson, H. Nakatsuji, M. Hada, M. Ehara, K. Toyota, R. Fukuda, J. Hasegawa, M. Ishida, T. Nakajima, Y. Honda, O. Kitao, H. Nakai, M. Klene, X. Li, J. E. Knox, H. P. Hratchian, J. B. Cross, C. Adamo, J. Jaramillo, R. Gomperts, R. E. Stratmann, O. Yazyev, A. J. Austin, R. Cammi, C. Pomelli, J. W. Ochterski, P. Y. Ayala, K. Morokuma, G. A. Voth, P. Salvador, J. J. Dannenberg, V. G. Zakrzewski, S. Dapprich, A. D. Daniels, M. C. Strain, O. Farkas, D. K. Malick, A. D. Rabuck, K. Raghavachari, J. B. Foresman, J. V. Ortiz, Q. Cui, A. G. Baboul, S. Clifford, J. Cioslowski, B. B. Stefanov, G. Liu, A. Liashenko, P. Piskorz, I. Komaromi, R. L. Martin, D. J. Fox, T. Keith, M. A. Al-Laham, C. Y. Peng, A. Nanayakkara, M. Challacombe, P. M. W. Gill, B. Johnson, W. Chen, M. W. Wong, C. Gonzalez, J. A. Pople. Gaussian, Inc., Wallingford, CT (2004).
31. W. Winter, T. Butters. *Acta Crystallogr., B* **37**, 1524 (1981).
32. E. Vogel, H.-W. Engels, S. Matsumoto, J. Lex. *Tetrahedron Lett.* **23**, 1797 (1982).
33. M. Randić. *Pure Appl. Chem.* **55**, 347 (1983).
34. E. Clar. *Polycyclic Hydrocarbons*, Vols. 1 and 2, Academic Press, London (1964).
35. E. Clar. *The Aromatic Sextet*, John Wiley, Chichester (1972).
36. H. Hosoya. *Top. Curr. Chem.* **153**, 255 (1990).
37. A. Ciesielski, T. M. Krygowski, M. K. Cyrański, M. A. Dobrowolski, J.-I. Aihara. *Phys. Chem. Chem. Phys.* **11**, 11447 (2009).
38. Z. Chen, C. S. Wannere, C. Corminboeuf, R. Puchta, P. v. R. Schleyer. *Chem. Rev.* **105**, 3842 (2005).